Ratchet dynamics of large polarons in asymmetric diatomic molecular chains



2010 J. Phys.: Condens. Matter 22 155105

(http://iopscience.iop.org/0953-8984/22/15/155105)

J. Phys.: Condens. Matter **22** (2010) 155105 (9pp) doi:10.1088/0953-8984/22/15/155105

# Ratchet dynamics of large polarons in asymmetric diatomic molecular chains

**L S Brizhik[1], A A Eremko[1], B M A G Piette[2] and W J Zakrzewski[2]**

[1] Bogolyubov Institute for Theoretical Physics, 03680 Kyiv, Ukraine
[2] Department of Mathematical Sciences, University of Durham, Durham DH1 3LE, UK

E-mail: brizhik@bitp.kiev.ua, eremko@bitp.kiev.ua, B.M.A.G.Piette@durham.ac.uk and W.J.Zakrzewski@durham.ac.uk

Received 23 October 2009, in final form 18 January 2010
Published 9 March 2010
Online at stacks.iop.org/JPhysCM/22/155105

**Abstract**

We study the dynamics of large polarons in diatomic molecular chains, at zero temperature, under the influence of an external, periodic in time, electric field of zero mean value. We show that in asymmetric chains, i.e. chains with two different atoms per unit cell, a harmonic unbiased field causes a drift of such polarons. Such a drift current, known as the ratchet phenomenon, depends strongly on the parameters of the chain; in particular, on the extent of the anisotropy of the chain and on the size of the polaron. Moreover, the drift takes place only if the intensity and the period of the field exceed some critical values which also depend on the parameters of the chain. We show that this directed current of polarons is a complicated phenomenon. It takes place in dissipative systems with a broken spatial symmetry and is generated by the interplay between the Peierls–Nabarro barrier and the impact of the external field on the charged polarons. The dependence of the amplitude of the polaron oscillations, the size of the drift per period of the external field and the average velocity are determined as a function of the intensity of the field and of its frequency.

(Some figures in this article are in colour only in the electronic version)

## 1. Introduction

The ratchet effect describes the appearance of a directed current (drift) of charged particles under the action of stochastic or deterministic unbiased (zero mean) ac forces [1]. It plays an important role in technical applications and is very important for understanding the functioning of biological motors. It is also generally accepted that this phenomenon has promising applications in nanotechnologies, including molecular motors and ratchets [2–6].

It is known that the necessary conditions for the ratchet effect under the action of stochastic or deterministic external forces, both in classical and quantum systems, involve energy dissipation in the system and the breaking of spatial and/or temporal symmetries [1]. Some of the necessary requirements for the ratchet effect are naturally intrinsic to molecular systems [7]. In particular, quasi-one-dimensional (quasi-1D) molecular chains with an intermediate value of the electron–phonon coupling support the existence of electron self-trapped states, usually referred to as polarons [7–11]. The class of low-dimensional molecular systems in which such polarons exist is quite large and includes quasi-1D organic and inorganic compounds (e.g. conducting platinum chain compounds), conducting polymers (such as polyacetylene, polypyrrole, polythiophene), as well as biological macromolecules ($\alpha$-helical proteins and DNA). In particular, energy dissipation in molecular systems is always present due to the interaction of atoms with the surrounding medium, as is the case, for instance, for biological macromolecules which are surrounded by the cellular cytoplasm. In molecular chains, due to their discreteness, polarons move in the Peierls–Nabarro potential which is periodic with a period equal to the spatial period of the lattice [12]. In spatially asymmetric molecular chains like, for instance, chains with a complicated structure, the Peierls–Nabarro potential is asymmetric and, therefore, it can play the role of the ratchet potential for the propagation of polarons under the influence of the external periodic field. Indeed, we have recently shown that an external non-biased (zero mean) periodic field, under certain conditions, can cause a drift of a polaron in molecular chains. This was reported first in our short paper [13] and in more detail in [14].

One problem with the polaron equations for specific systems is that some of the electron–phonon coupling

 

parameters have not been determined experimentally while others can only be estimated. Thus it makes sense to study the system by scanning a range of their values.

In this paper we report the results of our detailed study of the ratchet phenomenon in asymmetric diatomic molecular chains at zero temperature in large intervals of various parameter values. In particular, we show that the drift of polarons can take place when any of the anisotropy parameters, with the exception of mass, is non-zero, provided that the polaron is not too broad. We show that the drift of the polaron in this case results from its oscillations in the spatially asymmetric periodic Peierls–Nabarro potential when the system is subjected to both energy dissipation and a time-periodic non-biased electric field.

In section 2, we outline the derivation of the semi-classical equations for the asymmetric polaron system. In section 3, we describe how the polaron drift is altered when one varies various model parameters. In section 4 we briefly show that the collective coordinate approximation to our equations explains many of our numerical results. We finish the paper with some conclusions.

## 2. Hamiltonian of the system and dynamical equations

To study the ratchet phenomenon for molecular polarons, we consider the simplest case of a diatomic molecular chain in the nearest neighbour approximation, in the presence of an external periodic unbiased electric field at zero temperature. The state of an extra electron in such a system is described by the Fröhlich Hamiltonian which can be written in the form of a sum of three terms:

$$H = H_{\rm ph} + H_{\rm e} + H_{\rm e-ph}. \tag{1}$$

Here $H_{\rm ph}$ is the Hamiltonian of the lattice vibrations, $H_{\rm e}$ is the electron Hamiltonian and $H_{\rm e-ph}$ is the Hamiltonian that describes the electron–phonon interactions. For the numerical simulations it is convenient to use the Hamiltonian in the site representation.

In our asymmetric Hamiltonian, each coupling parameter will have two values: one for the intra-cell interactions, labelled s for *short*, and one for the cross-cell interactions labelled l for *long*. Let $z^0_{n,1} = na, z^0_{n,2} = na + b$ denote equilibrium positions of two different atoms or groups of atoms per unit cell, periodically arranged along the chain axis, with $a$ being the lattice constant and $b$ being the distance between the two atoms in a unit cell. The Hamiltonian of the lattice vibrations, $H_{\rm ph}$, in the harmonic approximation, is given by

$$H_{\rm ph} = \frac{1}{2}\sum_n \Bigg[\frac{p^2_{n,1}}{M_1} + \frac{p^2_{n,2}}{M_2} + w_{\rm s}(u_{n,1} - u_{n,2})^2 + w_{\rm l}(u_{n,1} - u_{n-1,2})^2\Bigg], \tag{2}$$

where $M_1$ and $M_2$ are the masses of the atoms, $u_{n,j}$ are the longitudinal displacements of the atoms from their equilibrium positions: $z_{n,j} = z^0_{n,j} + u_{n,j}$ and $p_{n,j}$ are the momenta, canonically conjugate to $u_{n,j}$. Finally, $w_{\rm s}$ and $w_{\rm l}$ are the elasticity constants between neighbouring atoms.

Introducing creation and annihilation operators of an electron on the site $(n, j)$, $a^\dagger_{n,j}$, $a_{n,j}$, respectively, the electron Hamiltonian can be written as

$$H_{\rm e} = \sum_n [\mathcal{E}_1 a^\dagger_{n,1}a_{n,1} + \mathcal{E}_2 a^\dagger_{n,2}a_{n,2} - J_{\rm s}(a^\dagger_{n,1}a_{n,2} + a^\dagger_{n,2}a_{n,1}) - J_{\rm l}(a^\dagger_{n,1}a_{n-1,2} + a^\dagger_{n-1,2}a_{n,1})], \tag{3}$$

where $\mathcal{E}_j$ is the on-site electron energy which includes the influence of the neighbouring atoms; $J_{\rm s}$ and $J_{\rm l}$ are the energies of the hopping interactions with neighbouring atoms.

The electron–phonon interaction Hamiltonian, $H_{\rm e-ph}$, results from the dependence of $J_{\rm s}$, $J_{\rm l}$ and $\mathcal{E}_j$ on the inter-atomic separation and, within the linear approximation with respect to the lattice displacements, is given by

$$H_{\rm e-ph} = \sum_n [a^\dagger_{n,1}a_{n,1}[\chi_{\rm l}(u_{n,1} - u_{n-1,2}) - \chi_{\rm s}(u_{n,1} - u_{n,2})] + a^\dagger_{n,2}a_{n,2}[\chi_{\rm l}(u_{n+1,1} - u_{n,2}) - \chi_{\rm s}(u_{n,1} - u_{n,2})]]. \tag{4}$$

Here $\chi_{\rm s}$ and $\chi_{\rm l}$ are the coefficients of the electron–phonon interaction between adjacent atoms.

For the numerical simulations it is convenient to use dimensionless units; thus, we introduce time measured in units of $\hbar/J$, energy measured in units of $J$ and displacements measured in length units $L = \hbar\sqrt{2/JM}$. We also introduce the following dimensionless parameters:

$$J = J_{\rm s} + J_{\rm l}, \qquad M = M_1 + M_2,$$
$$W = w_{\rm s} + w_{\rm l}, \qquad \chi = \chi_{\rm s} + \chi_{\rm l}, \qquad G = \frac{XL}{2J}, \tag{5}$$
$$C = \frac{\hbar^2 W}{MJ^2}, \qquad D = \frac{\mathcal{E}_2 - \mathcal{E}_1}{J}.$$

$$M_{1,2} = \tfrac{1}{2}M(1 \pm m), \qquad w_{\rm s,l} = \tfrac{1}{2}W(1 \pm w),$$
$$J_{\rm s,l} = \tfrac{1}{2}J(1 \pm d), \qquad \chi_{\rm s,l} = \tfrac{1}{2}X(1 \pm x). \tag{6}$$

By evaluating the Hamiltonian functional $\langle\Psi|H|\Psi\rangle$, we obtain the system of equations

$$\mathrm{i}\frac{\mathrm{d}\Psi_{n,1}}{\mathrm{d}t} = \Big[-1 + \frac{D}{2} + E(t)(n - n_0)\Big]\Psi_{n,1} + \tfrac{1}{2}(1 + d)\Psi_{n,2} + \tfrac{1}{2}(1 - d)\Psi_{n-1,2} + G[(1 + x)(u_{n,1} - u_{n,2}) - (1 - x)(u_{n,1} - u_{n-1,2})]\Psi_{n,1}, \tag{7}$$

$$\mathrm{i}\frac{\mathrm{d}\Psi_{n,2}}{\mathrm{d}t} = \Big[-1 - \frac{D}{2} + E(n - n_0 + b)\Big]\Psi_{n,2} + \tfrac{1}{2}(1 + d)\Psi_{n,1} + \tfrac{1}{2}(1 - d)\Psi_{n+1,1} + G[(1 + x)(u_{n,1} - u_{n,2}) - (1 - x)(u_{n+1,1} - u_{n,2})]\Psi_{n,2}, \tag{8}$$

$$\frac{\mathrm{d}^2u_{n,1}}{\mathrm{d}t^2} = -\frac{C}{1 - m}[(1 + w)(u_{n,1} - u_{n,2}) + (1 - w)(u_{n,1} - u_{n-1,2})] + \frac{G}{1 - m}[2x|\Psi_{n,1}|^2 - (1 - x)|\Psi_{n-1,2}|^2 + (1 + x)|\Psi_{n,2}|^2] - \Gamma\frac{\mathrm{d}u_{n,1}}{\mathrm{d}t}, \tag{9}$$

$$\frac{d^2u_{n,2}}{dt^2} = \frac{C}{1+m}[(1+w)(u_{n,1}-u_{n,2}) + (1-w)(u_{n+1,1}-u_{n,2})] + \frac{G}{1+m}[-2x|\Psi_{n,2}|^2 + (1-x)|\Psi_{n+1,1}|^2 - (1+x)|\Psi_{n,1}|^2] - \Gamma\frac{du_{n,2}}{dt}, \quad (10)$$

where we have added an external electric field $E(t)$, measured in units $ea/J$, as well as a dissipation term with coefficient $\Gamma$.

If we consider smooth and stationary solutions, $\frac{du_{n,j}}{dt} = 0$, of the system of equations (7)–(10) with $E = 0$ then one can show that the equations for $\Psi_{n,j}$ become, approximately, the discrete nonlinear Schrödinger equation with a cubic nonlinearity. To do this we must integrate the equations for the displacement fields by adding the equations (9) and (10) for all values of $n > k$. Using the fact that for large $n$, $\Psi_{n,j} = 0$ and that the displacements $u_{n,j}$ are constants, one obtains

$$u_{n-1,2} - u_{n,1} = \frac{G(1-x)}{C(1-w)}(|\Psi_{n-1,2}|^2 + |\Psi_{n,1}|^2), \qquad u_{n,1} - u_{n,2} = \frac{G(1+x)}{C(1+w)}(|\Psi_{n,1}|^2 + |\Psi_{n,2}|^2), \quad (11)$$

which can be substituted into (7) and (8) to get a discrete version of the nonlinear Schrödinger equations for the fields $\Psi_1$ and $\Psi_2$. Assuming $b = a/2$ we move to a continuum wavefunction by taking $\Psi_{n,1} = \Psi(x)$ and $\Psi_{n,2} \approx \Psi(x) + a\frac{d\Psi}{dx} + \frac{a^2}{2}\frac{d^2\Psi}{dx^2}$. After this transformation we obtain the standard nonlinear Schrödinger equation which admits the solution [13]

$$\Psi_{n,j}(t) = \sqrt{\frac{(1-P)\kappa a}{4}}\frac{\exp(-i\mathcal{E}_s t/\hbar)}{\cosh\kappa(z_{n,j}-R)}, \quad (12)$$

where $\mathcal{E}$ and $R$ are the eigenenergy and the centre of mass coordinate (cmc) of the polaron, respectively and the localization parameter of the polaron, $\kappa$, is given by

$$\kappa = (1-P)\frac{4G^2(1+x^2-2xw)\sqrt{1+D^2/4}}{aC(1-d^2)(1-w^2)}. \quad (13)$$

In (12) and (13) we have also introduced $P$ which is the weight of the contribution of the energy sub-levels of the upper band to the formation of the polaron state, split from the lower band bottom, taking into account that the polaron energy lies below the bottom of the lower electron band and is given by

$$\mathcal{E}_s = E_0 - \frac{\sqrt{\Delta_0^2 + 4J^2}}{2} - \frac{\kappa^2 J_s J_1 a^2}{\sqrt{\Delta_0^2 + 4J^2}}, \quad (14)$$

where $\Delta_0 = (\mathcal{E}_1 + \mathcal{E}_2)/2$. For the parameter range studied in this paper $P \ll 1$.

## 3. Results of the numerical simulations of the ratchet of polarons

As shown in [14], the existence of the polaron ratchet is due to the Peierls–Nabarro barrier experienced by the polaron propagating on a discrete lattice [12, 15–17]. This barrier, for an asymmetric diatomic lattice, is spatially asymmetric [14] and so it can play the role of the ratchet potential. Therefore, in all our simulations we have kept at least one asymmetry parameter non-zero. The height of the barrier depends on the extent of the polaron localization. From (12)–(13) we see that, in the case of a very weak anisotropy of the chain parameters, the polaron inverse width, in adimensional units, is $l_s^{-1} \propto 4G^2/C$. Following [14] we have set $C = 0.22$ in all our simulations. Hence, from now on, we refer to the parameter $G$ as 'the polaron width parameter'. Moreover, our results were obtained for the parameter values $D = 0.1$, $\Gamma = 0.2$, $b = 0.5$, and we varied the value of the polaron width parameter, $G$, in the interval [0.3–0.5]. These values were chosen so that they correspond to the values at which the polaron is neither too narrow, nor too broad, and are close to the realistic parameter values for the $\alpha$-helical proteins [18]. The values of the anisotropy parameters $x, d, w, m$ were also varied in a small range around 0.

For the numerical simulations we have considered a chain of 200 sites and have assumed quasi-periodic boundary conditions: when a localized polaron was close to one of the ends of the chain, it was automatically shifted by 130 sites towards the centre of the grid. This gave us a significant saving of computer time and has essentially generated the absence of the boundary effects on the dynamics of the electron. As a matter of fact, for most of our simulations, the automatic shift was not necessary as the polaron rarely reached the edge of the grid. In the simulations, we used as the initial condition a stationary solution of equations (7)–(10), obtained using a relaxation method, for the desired values of the model parameters but with the electric field set to zero, $E(t) = 0$.

According to [13] the ratchet effect in anisotropic chains can be induced by periodic time-symmetric ac field—so we have chosen the harmonic field $E(t) = E_0 \sin(2\pi t/T)$. We have then performed several sets of numerical simulations for various values of the asymmetry parameters. From our previous studies we know that the dynamics of the polaron is a very complicated combination of several oscillating processes with a phase diagram depending on many parameters of the system complicated by a combination of different domains corresponding to the absence or presence of the ratchet in the system and to the drift direction. Hence in our studies we have, first, taken as non-zero only one anisotropy parameter with all the others being equal to zero.

As we have shown in [14], polarons manifest their ratchet behaviour when the intensity of the field and their period exceed some critical values, $E_0 > E_{0,\mathrm{crit}}$, $T > T_{\mathrm{cr}}$. If the external force is very weak and its period is very small, the frequency of the polaron oscillations within the potential well of the Peierls–Nabarro barrier is very high and the amplitude of these oscillations is very small, $A \propto E_0 T^2 \ll a$, so that the polaron cannot overcome the intersite distance and remains pinned. Therefore, under such conditions the polaron cannot drift. To determine the polaron drift as a function of the intensity of the field, we set the period of the field large enough, so that the lattice deformation could follow the oscillations of the electron caused by the periodic force. Thus, for most of our calculations, we have chosen $T = 1000$ and $d = w = m = 0$.

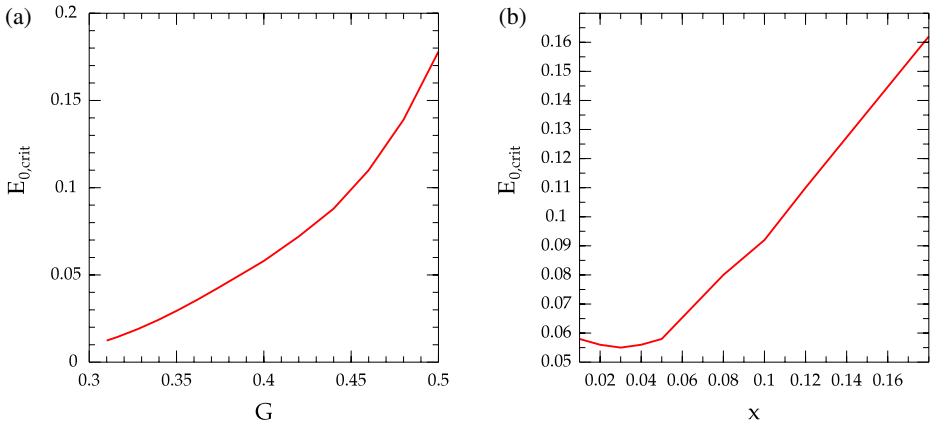


**Figure 1.** Dependence of the critical value of the electric field, $E_{0,\mathrm{crit}}$, on the polaron width parameter, $G$, for the case $x = 0.05$, $d = w = 0$ and (b) on the electron–phonon coupling asymmetry, $x$, for the case $G = 0.4$, $d = w = 0$.

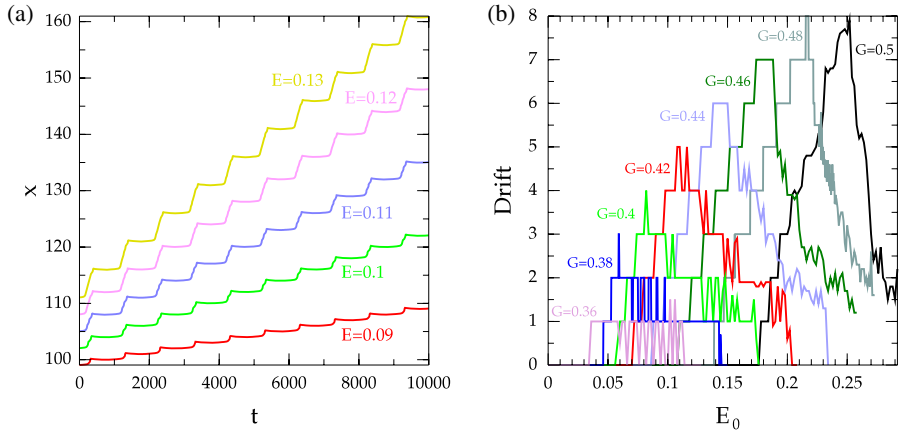


**Figure 2.** (a) Position of the cmc of the polaron as a function of time for $G = 0.36$ at $E_0 = 0.09$, $E_0 = 0.1$, $E_0 = 0.11$, $E_0 = 0.12$ and $E_0 = 0.13$, for $x = 0.05$, $d = w = 0$. The initial positions of the polarons have been shifted to avoid overlaps between the curves. (b) The amplitude of the polaron drift, for the case of $G$ varying from 0.36 to 0.5 with $x = 0.05$ and $d = w = 0$.

In figure 1 we present the critical value of the electric field, $E_{0,\mathrm{crit}}$, as a function of: (a) the polaron width parameter, $G$, for the case $x = 0.05$ and (b) of the electron–phonon coupling asymmetry, $x$, for the case $G = 0.4$. Notice that for small values of $x$, $E_{0,\mathrm{crit}}$ exhibits a plateau followed by a linear increase. This increase is explained by the fact that, as indicated by (13), the polaron is more localized when $x$ is non-zero. The Peierls–Nabarro potential is thus deeper and one requires a larger electric field to generate a drift.

The dependence of $E_{0,\mathrm{crit}}$ on the elasticity anisotropy parameter, $w$, is similar to the dependence on $x$, except that the drift is negative when $w > 0$ and the critical value of $w$ is $w_c = 0.06$.

Figure 2 presents our results on the drift of the polaron for several values of the electric field intensity. Namely, figure 2(a) shows the position of the cmc of the polaron as a function of time and figure 2(b) shows the amplitude of the polaron drift, i.e. the number of lattice sites that the polaron traverses during one period of the field, as a function of $E$. When the intensity of the field increases, the velocity and the amplitude of the polaron displacements increase too. However, when the field becomes very strong, the polaron begins to move very fast and radiates sound waves very intensively. In consequence, the effective polaron mass increases so much so that these two effects make the drift smaller. Above some upper critical value of the field, $E_0 > E_{\mathrm{cr},2}$ the polaron is destroyed—the electron undergoes a transition from the self-trapped state to a delocalized one. These upper critical values of the field correspond to the terminal points of the curves in figure 2(b). The destruction transition is very sharp and we will discuss this later.

The polaron drift is characterized by several parameters, such as the lowest and the upper critical values of the electric field, the largest drift value etc. All these characteristics depend on the width of the polaron and on the asymmetry of the Peierls–Nabarro barrier. It is very interesting that a relatively broad polaron manifests quite a regular pattern of its dynamics in a weak electric field, like, for instance, the polarons shown in figure 3.

It has been shown in [2, 19] that the uni-directional motion of the ratchet governed by equations of the type (20) corresponds to the limit cycle which is phase-locked to the frequency of the external driver: $R(t + T_c) = R(t) + na$, $\dot{R}(t + T_c) = \dot{R}(t)$. Here $a$ is the period of the ratchet potential

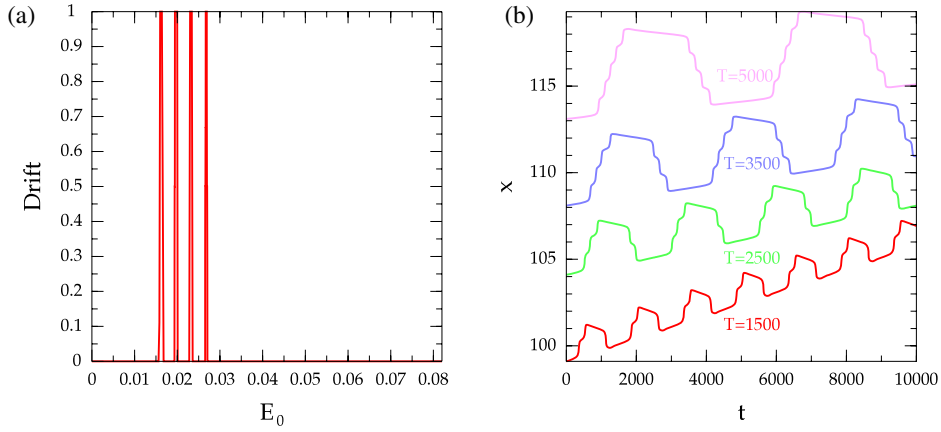


**Figure 3.** Amplitude of the polaron drift as a function of the intensity of the field for the parameter values $G = 0.32$, $x = 0.05$, $d = w = 0$: (a) drift for $T = 1000$; (b) trajectories of the cmc for $T = 1500$, $T = 2000$, $T = 2500$, $T = 3000$. The initial positions of the polarons have been shifted to avoid overlaps.

and $T_c$ is the period of the cycle. On this orbit, the average polaron velocity is given by

$$\langle V\rangle = \frac{1}{T_c}\int_0^{T_c} \dot{R}\,\mathrm{d}t = \frac{na}{lT_c} \tag{15}$$

with $n$ and $l$ being integers. In this resonance regime the polaron passes $n$ sites during $l$ periods of the external force and its profile, except for the shift in space by $n$ lattice periods, is reproduced after this time interval. And indeed, it has been shown in [14], that the polaron displacement is described by a piecewise linear function of the period of the external field with several plateaux, whose values satisfy the relation given by equation (15) and so correspond to the dynamical regimes that are limit cycles with numbers $n = 1, 2, \ldots; l = 1$ phase-locked to the driver. Therefore, the drift, expressed in lattice units, is expected to be given by the ratio of integers: $A_d = \langle V\rangle T/a = n/l$. This is indeed the case, as seen in our simulations and shown in figure 2.

The study of the polaron drift as a function of the intensity of the field for the case of a broad enough polaron has shown that there are 'windows' in the intensity of the field, when a polaron can drift by one lattice site per period. These results are shown in figure 3(a).

The amplitude of oscillations increases with the intensity of the field, so that the polaron drift consists of $m$ forward site steps followed by $l$ backward ones. In particular, in the case of a relatively strong electron–phonon interaction the polaron is relatively narrow and the drift gradually increases with the intensity of the field when $E$ is larger than some critical value $E_{crit}$ for the polaron drift. If the field is too strong, the polaron moves very fast and radiates sound waves so intensively that its drift becomes less and less regular and, as a result, the size of the drift decreases. For a field larger than some upper critical value, the polaron becomes unstable and undergoes a transition into a delocalized state. On the other hand, the relatively broad polaron (i.e. at a relatively weak electron–phonon coupling) exhibits a very interesting pattern of its drift. Namely, for a given period of the field oscillations above the corresponding critical value, the polaron can drift only when the intensities of the field belong to certain intervals, which are almost equally distributed. The number of such intervals, in other words the polaron 'drift windows', for a given polaron width, increases with the period of the field. The drift itself represents a movement of the polaron forward by $m$ sites and back by $l$ sites per period of the oscillating field. Here $m = 0, 0.5, 1, 1.5, \ldots$ and $l = 0, 0.5, 1, 1.5, \ldots$ such that $l \leqslant m$, and so the drift is equal to $d = m - l$. Note that in the chain there are two atoms per unit cell, so that such notation corresponds to the displacement of the polaron by a certain number of atoms along the chain. As the intensity of the field increases, $m$ increases too and $l$ becomes equal to $m - 1$ and, in consequence, we see that for a broad polaron $d = 1$. This can be seen from figure 3(b). In the case of a narrow polaron $l$ takes values in the interval $[0, m - 1]$ and so the drift takes values $d = 0, 1, 2, \ldots d_{max}$ increasing from 0 below the critical value of the field, to the value $d_{max}$ at the optimal intensity of the field and then decreasing again (as the intensity increases further). Here $d_{max}$ depends on the strength of the electron–phonon coupling (see figure 2(a)) and on the period $T$ as shown in figure 4 where we present the dependence of the drift and the critical value of the intensity of the field on the period of the field.

Finally, we compared the drift obtained when each of the anisotropy parameters are set separately to non-zero values. Some of our results are shown in figure 5. When $m = 0.1$, i.e. when the only anisotropy was induced by the mass, we observed no drift at all. The polaron oscillated around its initial position, but never drifted. When $w = 0.1$, the polaron drifted in the negative direction, as shown in figure 5. On the other hand, when we took $w = -0.1$, not shown, the polaron drifted in the positive direction. Looking at figure 5, we note that the drift patterns, apart from the negative drift for $w = 0.1$, are similar. At low field intensity, the polaron does not drift. When the field reaches a critical value, the polaron is able to drift and the drift increases with the field intensity up to a maximum value. If the field is increased further, the drift decreases and when the field is too strong, the polaron decays.

Another important observation that we can make as a result of our simulations involves pointing out the sharp

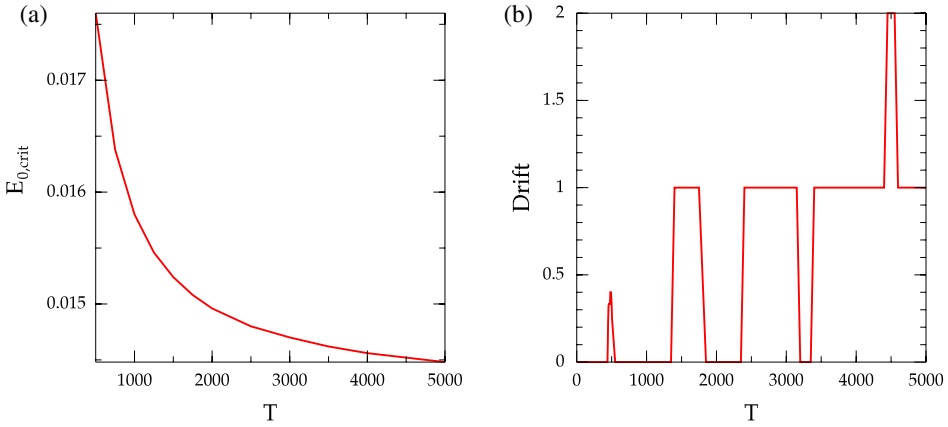


**Figure 4.** (a) Critical value of the electric field and (b) the polaron drift in the electric field $E_0 = 0.018$ as a function of the period of the field for the case $G = 0.32$, $x = 0.05$, $d = w = 0$.

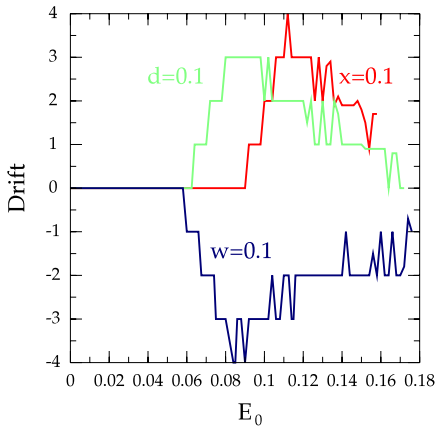


**Figure 5.** Amplitude of the polaron drift as a function of the intensity electric field for the case $G = 0.4$ and $x = 0.1$, $d = w = 0$; $w = 0.1$, $d = x = 0$; $d = 0.1$, $x = w = 0$.

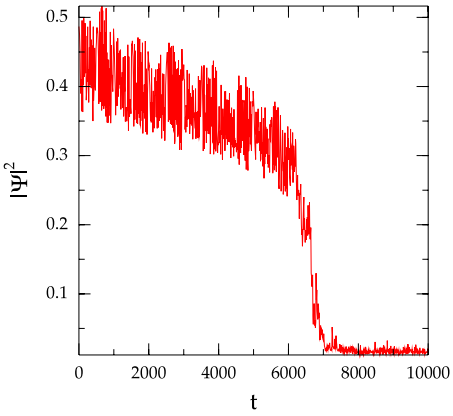


**Figure 6.** Maximum amplitude squared of the electron probability as a function of the intensity of the field with the period $T = 1000$ for the chain parameter values: $G = 0.36$, $D = 0.1$, $x = 0.05$, $w = d = 0$.

transition of the electron from a self-trapped polaron-like state into a delocalized state of an almost free electron. This is shown in figure 6 where we present the maximum value of $|\Psi|^2$ as a function of time. When the polaron is embedded in a strong electric field, it starts by widening until $|\Psi|^2 < 0.25$; then it undergoes a sharp decay into a delocalized state. The decrease of $|\Psi|^2$ in figure 6 is due to the widening of the polaron as it is progressively affected by the strong electric field.

## 4. Collective coordinate approximation

Some of the obtained numerical results can be understood in the collective coordinate approximation of equations (7)–(10) which one can also apply to discrete models [20, 21, 12]. We start by looking at the impact of the periodic field on a polaron in a chain with one atom per unit cell. As shown in [22, 23], a polaron in such a field oscillates with the frequency of the field and an amplitude of oscillations proportional to the amplitude of the field. Because of these oscillations the dynamical mass of the polaron in the external field is a function of the frequency of the field. As shown in [22, 23], there is a characteristic resonance frequency for a polaron, which is determined by the width of the polaron and the speed of sound in the chain (which sets the relaxation time of the chain):

$$\omega_{\rm res} = \frac{2\kappa V_{\rm ac}}{\pi}. \tag{16}$$

This resonance frequency defines three different regimes of polaron dynamics with an external periodic field: the low-frequency, high-frequency and resonance regimes. In the resonance regime, at $\omega \sim \omega_{\rm res}$, where $\omega$ is the frequency of the field, a polaron decays into a delocalized state by emitting phonons. In the high-frequency regime, when $\omega > \omega_{\rm res}$, the deformation created by the polaron cannot follow fast oscillations of the field, and, as a result, the dynamic mass of the polaron takes the value of the effective mass of an electron in the corresponding energy band, resulting in a trapped polaron. In the low-frequency regime, $\omega < \omega_{\rm res}$, the oscillations of the cmc of the polaron are accompanied by the oscillations of the local deformation of the chain and the dynamical mass of the polaron exceeds the effective mass of a

free electron and depends on $w$. In the limit of very small $w$ the dynamical mass of the polaron coincides with its effective mass in the absence of the field.

The height of the Peierls–Nabarro potential for a relatively broad polaron in a chain with one atom per unit cell is given by the expression

$$U_{\rm PN}(R) = U_0 \cos(2\pi R/b), \tag{17}$$

where $R$ is the position of the cmc of the polaron, $b$ is the lattice constant of the chain (in our notation $b = a/2$) and the height of the barrier depends on the electron–phonon coupling of the system [12]:

$$U_0 = \frac{4\pi^2 J}{\kappa b} \exp\left(-\frac{\pi^2}{2\kappa b}\right). \tag{18}$$

In a diatomic chain this barrier is also periodic but it has two components:

$$U_{\rm PN}(R) = U_1 \cos\left(2\pi\frac{R}{a}\right) + U_2 \cos\left(4\pi\frac{R+b}{a}\right), \tag{19}$$

making it asymmetric for an asymmetric chain. This barrier can thus play the role of the ratchet potential for the polaron in the presence of the external periodic field. Of course, as the positions of the atoms evolve with time, the Peierls–Nabarro potential changes and this, in turn, affects the drift of the polaron. Thus, we expect, that the drift of the polaron is possible, provided that the Peierls–Nabarro potential can follow the oscillations of the polaron, i.e. in the low-frequency fields. In the case of high-frequencies of the field the deformation cannot follow the oscillations of the polarons and, as a consequence, the Peierls–Nabarro potential cannot act as a ratchet potential and the polaron cannot drift. In [14] we showed that the resonance frequency of the polaron $\omega_{\rm res} = 2\pi/T_{\rm res}$ where $T_{\rm res} \approx 22$. This was confirmed by our numerical results which showed that the polaron drift takes place only if the period of the field exceeds some critical value (see figure 4).

For a broad enough polaron the collective coordinate approach is valid. In this case the dynamic equation for the polaron cmc in the presence of the external low-frequency field, $E(t)$, taking into account the Peierls–Nabarro potential and the energy dissipation, can be written in the form [12]:

$$M_{\rm s}\frac{{\rm d}^2R}{{\rm d}t^2} = \gamma\frac{{\rm d}R}{{\rm d}t} + f(R) + eE(t), \tag{20}$$

where $\gamma \propto \Gamma$ (see equations (7)–(10) in [24]), and $f(R) = -{\rm d}U_{\rm PN}/{\rm d}R$. First of all, note that the polaron moves with a velocity bounded from above by the sound velocity in the chain and by the group velocity of the electron in the conducting band. As for the fields considered here, this velocity is relatively small, the drift of the polaron is thus determined by its velocity. In the adiabatic regime, considered here, the second derivative of the polaron cmc is much smaller than the first derivative and in a first approximation can be omitted in equation (20). In this case for the harmonic fields $E(t) = E(t+T) = E_o \sin(2\pi t/T)$ and so equation (20) is invariant with respect to the rescaling $T \to \alpha T$, $\gamma \to \alpha\gamma$, where $\alpha$ is an arbitrary constant. Therefore, we expect such rescaling also for the drift properties of the broad polaron in the adiabatic regime. Amazingly, this prediction agrees very well with the results of our numerical simulations as shown in figure 7 for polaron parameters $G = 0.32, x = 0.05$ at $\Gamma = 0.1, T = 1000$ (a) and $\Gamma = 0.2, T = 2000$ (b) thus supporting our collective coordinate approximation.

## 5. Conclusions

In this paper we have investigated how the parameters of an asymmetric molecular chain, containing two different atoms per unit cell, affects the ratchet behaviour of polarons.

Our first observation is that if the only asymmetry of the chain comes from the atom masses, i.e. $m \neq 0$, then the polaron does not exhibit a ratchet behaviour. On the other hand, if any of the other asymmetry parameters, $d$, $w$ or $x$, are non-zero then the ratchet phenomenon is observed. A polaron on an asymmetric chain is, to leading order (see equation (13)), more localized than the equivalent symmetric polaron. As a result, the Peierls–Nabarro potential is deeper and one requires a larger electric field to induce a ratchet drift.

To be able to drift, a polaron has to be neither too broad nor too localized. In the former case, the polaron is spread over too many lattice sites to perceive the asymmetry of the chain while in the latter, the Peierls–Nabarro potential is so deep that the electric field required to move the polaron out of its well is so large that it destroys it.

To generate a polaron drift, one must use a time-symmetric electric field with a period $T$ much larger than the resonance period of the polaron ($T_{\rm res} \approx 22$ is our units). Once this condition is fulfilled, the polaron drifts by a fixed distance per period. The polaron average speed is thus larger for smaller values of the period $T$.

There is a large class of low-dimensional molecular systems, including biological macromolecules, conducting polymers and inorganic compounds, which possess large polarons, as has been seen in numerous experimental observations. In particular, molecular polarons, which in biological systems can be responsible for the charge and energy transfer during the metabolic processes [7], are formed in $\alpha$-helical proteins. Such protein macromolecules possess a highly asymmetric structure, and, therefore, their Peierls–Nabarro barrier is asymmetric. Therefore, in these systems the presence of symmetric stochastic noise can result in the formation of a directed current of polarons, i.e. such systems could be good candidates for molecular motors.

On the other hand, there is a class of low-dimensional compounds with an asymmetric unit cell, such as polyphenylene-venillene, polythienylene-venillene, etc, in which the existence of large polarons and bipolarons has been experimentally confirmed [25–27]. Based on our results we expect that, in these compounds, the unbiased alternating electric field can induce a directed current.

We expect that the ratchet effect can also take place in compounds with charge density waves (CDW) (see review [28]). Similarly to the case of polarons, such CDWs have also been studied within the adiabatic approximation

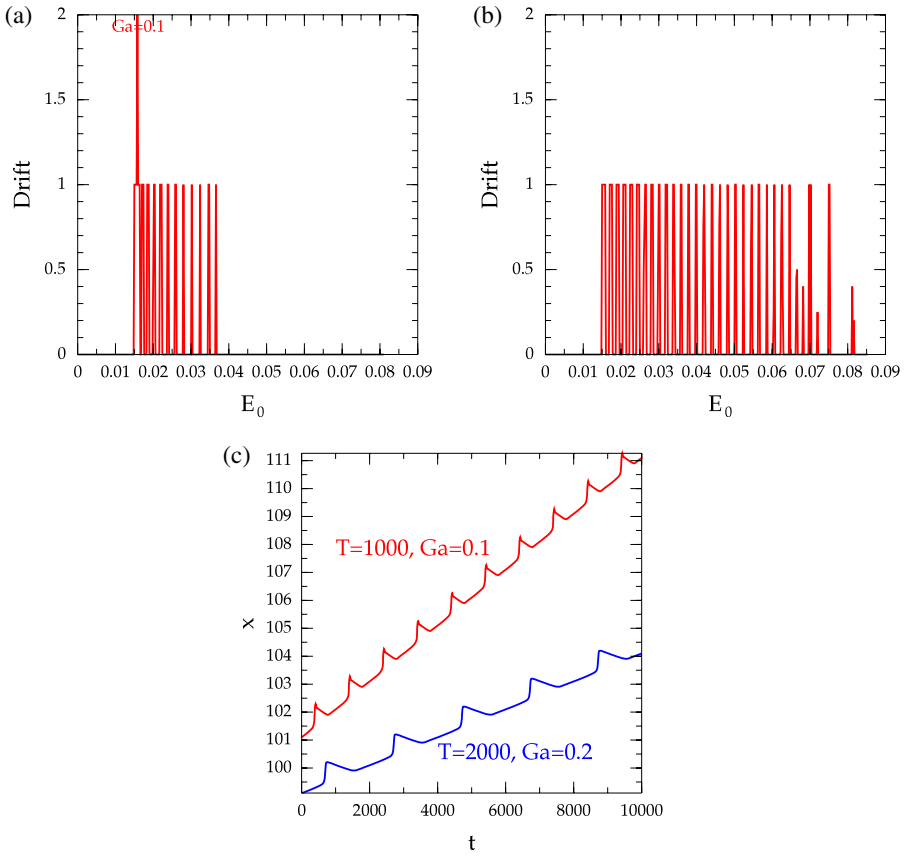


**Figure 7.** Amplitude of the polaron drift $G = 0.32$, $x = 0.05$ at $\Gamma = 0.1$, $T = 1000$ (a); $\Gamma = 0.2$, $T = 2000$ (b); position of the polaron as a function of time (c) $G = 0.32$, $x = 0.05$ at $\Gamma = 0.1$, $T = 1000$ and $\Gamma = 0.2$, $T = 2000$. The initial positions of the polarons have been shifted to avoid overlaps.

for the many-electron wavefunctions and, in the limit of low concentration of electrons, the CDW wavefunction reduces to the wavefunction of separated bipolarons [29], as was shown in [30]. Indeed, the dc signal produced by biharmonic microwaves in TTF-TCNQ (tetrathiofulvalene-tetracyanoquinodimethane) has been experimentally observed [31]. To explain some features of these experimental results, a CDW was modelled in [32] as a Brownian motion of a classical particle in a periodic potential within the collective coordinate approach, equation (20). This agrees qualitatively with our results, though a further detailed study still has to be performed.

We note that, similarly to the deterministic fields considered here, symmetric white noise [33] also can cause uni-directed current of polarons in low-dimensional molecular systems, though the dynamics of polarons in such cases is less symmetric and more complicated than in the harmonic fields. Moreover, our preliminary studies of such systems show that thermal noise can decrease the critical value of the intensity of the field. We plan to report on this in the near future.

## Acknowledgments

This work has been supported by a Royal Society travel grant. One of us, LSB, acknowledges the Grey College Fellowship, for the Easter term 2009. She thanks the College and the University for their hospitality.

## References

[1] Reimann P 2002 *Phys. Rep.* **361** 57
[2] Denisov S, Flach S, Ovchinnikov A A, Yevtushenko O and Zolotaryuk Y 2002 *Phys. Rev.* E **66** 041104
Flach S, Yevtushenko O and Zolotaryuk Y 2000 *Phys. Rev. Lett.* **84** 2358
Flach S, Zolotaryuk Y, Miroshnichenko A E and Fistul M V 2002 *Phys. Rev. Lett.* **88** 184101
Salerno M and Zolotaryuk Y 2002 *Phys. Rev.* E **65** 056603
[3] Ustinov A V, Coqui C, Kemp A, Zolotaryuk Y and Salerno M 2004 *Phys. Rev. Lett.* **93** 087001
[4] Zolotaryuk Y and Salerno M 2006 *Phys. Rev.* E **73** 066621
[5] Morales-Molina L, Quintero N R, Snchez A and Mertens F G 2006 *Chaos* **16** 013117
[6] Gorbach A V, Denisov S and Flach S 2006 *Opt. Lett.* **31** 1702
[7] Davydov A S 1985 *Solitons in Molecular Systems* (Dordrecht: Reidel)
[8] Su W P, Schrieffer J R and Heeger A J 1979 *Phys. Rev. Lett.* **42** 1698
Su W P, Schrieffer J R and Heeger A J 1980 *Phys. Rev.* B **22** 2099
[9] Rice M J, Phillpot S R, Bishop A R and Campbell D K 1986 *Phys. Rev.* B **34** 4139
[10] Rice M J and Phillpot S R 1987 *Phys. Rev. Lett.* **58** 937
[11] Heeger A J, Kivelson S, Schrieffer J R and Su W-P 1988 *Rev. Mod. Phys.* **60** 781

[12] Brizhik L, Cruzeiro-Hansson L, Eremko A and Olkhovska Yu 2000 *Phys. Rev.* B **61** 1129
Brizhik L, Cruzeiro-Hansson L, Eremko A and Olkhovska Yu 2003 *Ukr. J. Phys.* **43** 667
[13] Brizhik L, Eremko A, Piette B and Zakrzewski W 2008 *J. Phys.: Condens. Matter* **20** 255242
[14] Brizhik L S, Eremko A A, Piette B M A G and Zakrzewski W J 2009 Field driven current in nonlinear low-dimensional nanosystems *Environmental and Biological Risks of Nanobiotechnology, Nanobionics and Hybrid Organic-Silicon Nanodevices* (Berlin: Springer)
[15] Peierls R E 1940 *Proc. Phys. Soc. Lond.* **52** 23
[16] Nabarro F R N 1947 *Proc. Phys. Soc. Lond.* **59** 256
[17] Kuprievich V A 1985 *Physica* D **14** 395
[18] Brizhik L, Eremko A, Piette B and Zakrzewski W 2004 *Phys. Rev.* E **70** 031914
[19] Zaslavsky G M 1998 *Physics of Chaos in Hamiltonian Systems* (London: Imperial College Press)
[20] Braun O M and Kivshar Y S 1998 *Phys. Rep.* **306** 1
[21] Morales-Molina L, Quintero N R, Sanches A and Mertens F G 2006 *Chaos* **16** 013117
[22] Brizhik L and Eremko A 1997 *Phys. Alive* **5** 9
[23] Brizhik L, Cruzeiro-Hansson L and Eremko A 1999 *J. Biol. Phys.* **24** 223
[24] Davydov A A and Eremko A A 1980 *Teor. Mat. Fiz.* **43** 367 (in Russian)
[25] Bredas J L, Scott J C, Yakushi K and Street G B 1984 *Phys. Rev.* B **30** 1023
[26] Chung T-C, Kaufman J H, Heeger A J and Wudl F 1984 *Phys. Rev.* B **30** 702
[27] Wilson E G 1983 *J. Phys. C: Solid State Phys.* **16** 6739
[28] Grüner G 1988 *Rev. Mod. Phys.* **60** 1129
[29] Brizhik L S and Davydov A S 1984 *Sov. J. Low Temp. Phys.* **10** 748
Brizhik L S 1986 *Sov. J. Low Temp. Phys.* **12** 437
[30] Eremko A A 1992 *Phys. Rev.* B **46** 3721
Eremko A A 1994 *Phys. Rev.* B **50** 5160
[31] Seeger K and Maurer W 1978 *Solid State Commun.* **27** 603
[32] Wonneberger W 1979 *Solid State Commun.* **30** 511
[33] Luczka J, Bartussek R and Hänggi P 1995 *Europhys. Lett.* **31** 431
Luczka J, Czernik T and Hänggi P 1997 *Phys. Rev.* E **56** 3968